

This is the peer reviewed version of the following article:

González-Benito, J., Olmos, D., Teno, J. & González-Gaitano, G. (2019). Nanomorphology and nanomechanical characteristics of solution-blow-spun PVDF-based fibers filled with carbon nanotubes. *Journal of Applied Polymer Science*, 136(10), 47115,

which has been published in final form at

<https://doi.org/10.1002/app.47115>

This article may be used for non-commercial purposes in accordance with Wiley Terms and Conditions for [Use of Self-Archived Versions](#).

Nanomorphology and Nanomechanical Characteristics of Solution Blow Spun PVDF based Fibers when Filled with Carbon Nanotubes

Javier González-Benito^{1*}, Dania Olmos¹, Jorge Teno¹, Gustavo González-Gaitano²

¹ Dept. Materials Science and Engineering, IQMAAB, Universidad Carlos III de Madrid, Av. Universidad 30, 28911 Leganés, Madrid, Spain.

² Dept. Química, Facultad de Ciencias, Universidad de Navarra, 31080, Pamplona, Spain

Corresponding autor:

Javier González-Benito

Address: Av. Universidad 30, 28911 Leganés (Madrid – Spain)

e-mail: javid@ing.uc3m.es

ABSTRACT

Fibers of poly(vinylidene fluoride), PVDF, filled with multi-walled carbon nanotubes, MWCNT, were prepared by solution-blow-spinning, SBS. The influence of the MWCNT on the surface morphology and the mechanical behavior of single fibers were studied. The morphology of the materials prepared so as the dispersion of the MWCNT within the polymer were studied by optical microscopy, OM, and transmission electron microscopy, TEM. Atomic force microscopy, AFM, was used to inspect the topography of single fibers so as to perform nanoindentation tests. OM and TEM images suggested quite good dispersion of the MWCNT within the PVDF. AFM images clearly evidenced changes in the topography of the SBS fibers when the MWCNT were added to the PVDF. A greater amount of MWCNT in the PVDF led to more heterogeneous fibers surfaces. The nanoindentation force curves revealed that the stiffness was almost constant along the fibers, which indicated that the mechanical response was homogeneous and, in turn that the distribution of MWCNT should be uniform along the PVDF fibers. The incorporation of the MWCNT reinforced the PVDF fibers, showing increments of 31% and 49% in the elastic modulus when 1% and 5% by weight of MWCNT were added to the polymer respectively.

Keywords

PVDF; Solution blow spinning; MWCNT; properties at nanoscale; AFM.

INTRODUCTION

In order to ensure the proper performance of materials it is necessary to determine and, if possible, to control certain mechanical properties. Macroscopic properties are highly dependent on the microscopic or even the nanoscopic ones. Therefore, it is reasonable to think that the study of those properties at small scales should help to understand the origin of a particular macroscopic behavior to finally design materials efficiently.

On the other hand, materials are necessary sometimes for being used in certain circumstances where phenomena at nanoscale are the main origin of perturbations. As a consequence, performing mechanical tests at adequate scales should be compulsory. Clear examples of this refer, for instance, to those materials based on submicrometric fibers or small particles interconnected each other. If the behavior of these materials under the effect of certain events occurring at small scales is taken into account, there is a need of carrying out mechanical tests at micro or even at nanoscale. One example would be represented by a material whose dimensional change at nanoscale, due to their response to certain stimuli (cells adhesion and biofilm growing), is a very important characteristic to be controlled respect to certain applications, for instance, tissue engineering.^{1,2}

There are several works that confirm a direct relation between mechanical properties of materials, microorganisms adhesion and subsequent biofilm formation.³⁻⁸ It is generally accepted that, among the materials properties, the stiffness is one of the least explored respect to its effect on the bacterial adhesion.¹ For example, Kamimura et al., using gel substrates with a photoactivable surface, demonstrated differences in the collective migration behavior of cell clusters depending on the substrate stiffness.³ Huang et al.⁴

developed a mechano-chemical coupling model to physically describe cell adhesion and spreading mediated by substrate stiffness. Brown et al.⁵ have correlated the mechanical and surface properties of polydimethylsiloxane to vascular smooth muscle cells behavior finding that, in the absence of serum, there is a remarkable decrease in both cell attachment and spreading as the elastic modulus of the substrate decreases from 1.79 to 0.05 MPa. Likewise, Yeung et al. have reported a clear influence of substrate stiffness on fibroblasts, endothelial cells, and neutrophils morphology, cytoskeletal structure, and adhesion.⁶ Tee et al. using microcontact printing and microfabricated arrays of elastomeric posts showed that cell cortical stiffness increased as a function of both substrate stiffness and spread area.⁷

The reasons usually given for that direct relation between mechanical properties of a particular substrate and the microorganisms attachment with their subsequent development are related to the substrate material ability to be deformed under relatively low stresses of the order of tens of nano-Newtons. These mechanical stresses may arise from surrounding perturbations such as changes in the environmental conditions or the simple activity of the microorganisms. Due to this, it seems reasonable to study the properties of the materials at small enough scale in order to be able to extrapolate their results to the final materials behavior or performance at a similar dimensional scale.

Although a particular material can be prepared with dimensions above the micro-scale, many times it can be constituted by submicrometric elements that, after certain arrangement, provide macroscopical integrity. This would be the case of mats formed by submicrometric fibers generated in processes such as electrospinning⁹⁻¹¹ or solution blow spinning, SBS.^{12,13} **Therefore, the necessity of studying the mechanical properties**

of those small elements is evident, at least because of two reasons: a) the macroscopic properties of the whole material can depend on them and b) they might influence processes occurring at small scales, like cell adhesion and spreading. One example of the later can be found when these mentioned fibrous materials have potential use in, for example, tissue engineering, wound healing, etc.

In the present work a system formed by the combination of poly(vinylidene fluoride) and multi-walled carbon nanotubes has been chosen because of the interesting well known electromechanical properties of the PVDF.^{14,15} Besides, carbon nanotubes reinforced PVDF nanocomposites have shown improvements in the mechanical, thermal, and electrical properties compared to those of the neat PVDF.¹⁶ On the other hand, carbon nanotubes are conductive particles so when they are added to a polymer they should change the electrical properties of the polymer. Therefore, electromechanical properties of the PVDF are expected to be highly influenced by the presence of highly conductive nanoparticles as the MWCNT. These particular behaviors are especially important if proliferation of certain cells is wanted to be controlled by electromechanical stimulation.¹⁷

In the last decade some articles have shown the usefulness of atomic force microscope to extract mechanical information at nanoscale of submicrometric fibers. In fact, some review¹⁸ deal with experimental methods to test single polymeric submicrometric fibers at nanoscale, for example tensile test¹⁹, three-point bend test²⁰ and indentation test. Mechanical properties such as Young's modulus, stress and strain at break of a single ultrafine fiber can then be obtained from these tests.¹⁸ Among those different methods perhaps that one based on indentation of single fibers may have more advantages. In the

other cases, the assumption of good adhesion between the fiber and the substrate might not be correct if fiber slipping is not avoided under the loads applied parallel to the substrate during the mechanical tests. For the nanoindentation test, a fiber is deposited on a substrate with a very smooth surface and an AFM tip is used to indent the fiber. Therefore, the sample preparation for this test seems to be easier.

By the use of an AFM the present work aims to study the general morphology, topography and the mechanical response at nanoscale of single fibers of poly(vinylidene fluoride) produced by SBS. The influence of the presence of multi-walled carbon nanotubes within the polymer was analyzed. In this work three compositions in terms of MWCNT were chosen: 0%, without MWCNT; 1%, with MWCNT but below the percolation threshold and 5%, relatively low concentration but well above the percolation threshold.

EXPERIMENTAL

Materials

Poly(vinylidene fluoride), PVDF, supplied by Sigma-Aldrich ($M_n = 10.700$; $M_w = 27.500$; density 1.78 g/cm^3) was used as the polymer matrix. Multi-walled carbon nanotubes, MWCNT, were used as the nanofiller (Sigma-Aldrich; carbon content $> 95 \text{ wt\%}$, 6 to 9 nm in diameter and $55 \mu\text{m}$ length, density 2.1 g/cm^3). Dimethylformamide, DMF, and acetone, Ac, HPLC grade (Sigma-Aldrich) were used as the solvents for the solutions and suspensions to be blow spun.

Samples preparation

Solutions and suspensions to be blow spun were prepared using a mixture of DMF/Ac 1:9 (v/v), adding the required amount of polymer as to finally have mixtures with a composition of 11% (wt/v) of PVDF. To prepare the suspensions a particular amount of MWCNT was firstly added to 4 mL of the DMF/Ac mixture, sonicated for 15 min and finally added to a PVDF solution in DMF/Ac. Three mixtures were prepared with different weight percentages of nanotubes, 0%, 1% and 5%, respectively.

To produce the PVDF fibers a home-made SBS equipment inspired by the device patented by Medeiros et al.¹² was used. Basically, the device is composed by a nozzle connected to an air compressor with a pressure regulator and a plastic syringe coupled to an automatic pump (NE 1000 X, New Era System, Inc., Farmingdale, NY). The nozzle consisted of an aluminum tube (inner diameter 0.7 mm) with a hole to blow air at 4 bars. Along the aluminum tube a glass capillary (inner diameter 0.5) was introduced and positioned so it protruded 2 mm beyond the aluminum cylinder. The mixture formed by the solvent, the polymer and the MWCNT was pumped at 0.5 mL/min and ejected from the nozzle, to finally be deposited on a rotating cylindrical collector wrapped with aluminum foil and located at 15 cm of working distance. In the Figure 1 a picture of the experimental setup used in this research is shown.²¹

Figure 1.

Equipments

The morphology of the blow spun samples was studied by optical microscopy, OM, using an opto-digital microscope OLIMPUS DSX500 to see nanotube dispersion at microscale. The location and distribution at nanoscale of the MWCNT within the PVDF

polymer were carried out by transmission electron microscopy, TEM, using a Philips Tecnai 20F FEG analytical microscope operating at 200 kV.

Topography, phase contrast and amplitude images of single fibers were obtained by AFM under the tapping mode with an atomic force microscope (Nanoscope IV, veeco instruments) using silicon tips of force constant 42 N/m. The arithmetic mean height, R_a , root mean square average height, R_{ms} , the mean roughness depth, R_z and the maximum roughness depth, R_{max} were chosen as the roughness parameters for the topographic characterization.

Force curves of the materials were obtained from indentations on single fibers using the same tip used to obtain the images. After selecting the position of the indentation, just in the highest part of the fiber (Figure 2), loads lower than 2000 nN were applied to finally obtain indentation plots, corresponding to the cantilever deflection in terms of the force applied (in nN) versus the tip-sample indentation (in nm).

Figure 2.

RESULTS AND DISCUSSION

In the Figure 3 images obtained by an optical profilometer are shown for the PVDF with and without nanotubes respectively.

Figure 3.

In all cases transparent fibers with diameters of hundreds of nanometers were obtained together with lumps of about 10 μm . As can be seen, when the MWCNT are added to the polymer, dark regions well spread out are observed. It is also important to highlight that the darkest regions are coincident with those where more material is accumulated or where the lumps are located. In order to better visualize the dispersion of the MWCNT within the polymer, at least at the resolution of the optical microscope, a zoomed region of the image for the sample with 5% by weight of MWCNT is presented in Figure 4. It can be observed how the dark spots can be found in the whole material and mainly distributed all along the fibers which suggest a good dispersion of the MWCNT throughout the fibers.

Figure 4.

However, taken into account the small dimensions of the MWCNT the information about the dispersion would more complete if higher resolution techniques were used. In the Figure 5 a TEM image is shown where part of a PVDF fiber filled with 1% by weight of MWCNT is observed. It seems that the MWCNT are located in an extended way along the PVDF fiber. Although at microscale higher concentration of MWCNT can be observed in the regions with more accumulation of material (lumps), it seems that the dispersion of MWCNT at nanoscale is quite uniform. This result does not mean that the dispersion of MWCNT was perfect. In order to have MWCNT perfectly or uniformly dispersed it would be necessary to identify all the nanotubes completely isolated. Attending the concentrations used so as the shape and dimensions of the MWCNT the probability of contacts between them is very high. Therefore, even at concentrations lower than 1% anyone would expect regions with slight variations in the

nanotubes content. A possible way of improving or perhaps avoiding these contacts might be the surface modification of the MWCNT.

Figure 5.

On the other hand, as an example, AFM images of topography, phase contrast and amplitude so as the corresponding cross section profile of one fiber are represented in the Figure 6 (representative blow spun fiber of PVDF filled with 1% wt of MWCNT). Regardless of the composition of the samples, almost cylindrical fibers were obtained with diameters shorter than 400 nm.

It is well known that the motion of AFM probe in the tapping mode is characterized by its phase relative to a driving oscillator, changing the phase signal when the probe encounters regions of different mechanical response. The phase contrast image in the Figure 6 (top, left) shows that there is not any change in the phase signal of the AFM tip. This result suggests that, for a particular composition of the materials under study, differences on the mechanical response along the fibers do not exist; in other words, the introduction of MWCNT does not lead to heterogeneity in terms of stiffness along the fibers.

From the topographic images, as that one shown in the Figure 6 (bottom-left), some morphological and topographical parameters can be obtained. One of the most common surface properties that can be studied is the roughness of the fibers. Several roughness parameters can be extracted from linear profiles. The values of those roughness

parameters obtained for all the materials under study are gathered in the Table 1. It can be observed that, in terms of morphology, the higher amount of MWCNT within the PVDF the more heterogeneous the surfaces of the fibers are. Besides, as can be reflected by the values of the roughness parameters (Table 1), the fibers with MWCNT presented rougher surfaces. Furthermore, it can be observed that when the nanofiller content increases from 1% to 5% by weigh the roughness also increases. Here, it is important to highlight that, in terms of adhesion; this result may have important repercussions on the fibers surface behavior.

Figure 6.

Table 1.

In the Figure 7, as an example, a typical indentation force curve obtained in a single blow spun PVDF fiber is represented. The first part of the curve, for which 0 nN of load was applied, represents the tip approaching towards the sample. The contact between the tip and the sample is represented as the origin in terms of indentation displacement (0 nm). After that, there is a linear region of constant increase of the load applied, that arises from a constant change of the cantilever deflection and that can be the consequence of the elastic behavior of the fiber. At around 40 nm of indentation there is a change in the slope of the force curve and that suggests the existence of plastic deformation. Then, at 90 nm of indentation the deflection or the applied load remains almost constant, pointing out the existence of mechanical failure of the fiber at an indentation of about 70 %. Finally, it can be seen that for an indentation of 110 nm, very close to the diameter of the fiber (135 nm) used as the specimen for the indentation test,

there is a very sharp increase of the slope of the force curve which, in fact, is coincident with the slope obtained for the force curve of the very hard material used as substrate (mica). This result suggests that the PVDF fiber was broken by the tip, sectioning it to finally reach the mica substrate.

In order to gather information about the stiffness of the different materials under study, the elastic parts of the indentation curves were used to make comparisons (Figure 8). Several authors have shown that typical stress-strain tests of PVDF based materials gave force curves for which the plastic deformation was attained at deformations lower than the 5%.¹⁴ In particular, for the tested fibers with diameters in the range 100 to 400 nm, 5% of deformation would correspond to a range of indentation between 5 to 20 nm. Therefore, to compare mechanical responses of the samples from the indentation curves only the elastic part for which the indentation is less than 20 nm was taken into account (Figure 8).

Figure 7.

Figure 8.

As can be seen, the slopes of the force curves largely depend on the composition of the sample. If it is assumed, as expected, a higher slope for a stiffer material, the mica should be the stiffest material since the highest slope was obtained for it. Then, comparing the PVDF based materials it can be observed a trend in the slopes of the indentation curves that depends on the MWCNT content. The slopes are higher the higher the amount of the nanofiller is. These results point out therefore that the higher

the nanotubes content the higher the stiffness, in accordance with the reported results that were obtained by performing other mechanical tests, such as conventional strain-stress tests which give macroscopic information.^{14,22} Besides, taking into account that the fibers under study have similar values of roughness and curvatures and that they should have similar contribution from possible existence of adhesion forces (other factors that may affect indentation curves),¹⁸ it can be concluded that the incorporation of carbon nanotubes reinforces at nanoscale the PVDF which, finally must be the main cause of the corresponding macroscopic mechanical reinforcement.

Considering negligible the effect of underlying substrate, the ambiguity of the tip shape (it is assumed a spherical indenter), that the indentation is performed perfectly perpendicular to the surface of the fiber and that there is not any adhesion force effect, a very simple estimation of the indentation modulus of the fibers studied can be done. In particular, knowing the value of the elastic modulus of the mica, by comparison, a value of the indentation modulus of the fibers is possible to be estimated. For a perfect elastic behavior of the cantilever, its deflection should be directly proportional to the tip-sample indentation curve during the elastic behavior of the material; therefore, the proportionality constant, H ($H = C \cdot E$, where C is a constant dependent on the equipment conditions), or the slope of the force curve, must be, at the same time, directly proportional to the elastic modulus, E

$$Deflection(nN) = H \cdot Indentation(nm) \quad (1)$$

Thus, by simply comparing the force curves and knowing the elastic modulus of one material an estimation of the elastic modulus, E , of any material can be done. Taking

into account that the elastic modulus of the mica is well known, $E_M = 171 \text{ GPa}$,²³ it can be deduced from eq. (1) that

$$\frac{Slope_{Mica}}{Slope_{Material}} = \frac{H_{Mica}}{H_{Material}} = \frac{C \cdot E_{Mica}}{C \cdot E_{Material}} = \frac{E_{Mica}}{E_{Material}} \quad (2)$$

From eq. 2 an estimated value of 2 GPa for the elastic modulus of the PVDF was obtained. This value is quite coincident to those reported in several works¹⁴, although they were obtained at a macroscopic scale. Therefore, this result suggests, at least for these materials, a correspondence or a clear proportional relation between the mechanical responses at nano and macro scales. Following with the same simple estimations, when only 1% by weight of MWCNT was incorporated to the SBS PVDF fibers an increment of 31% in the modulus of a single fiber was obtained while, when 5% of MWCNT is added to the polymer, an increment of 49% was obtained, reflecting the effectiveness of the incorporation of MWCNT via SBS process to reinforce the PVDF.

CONCLUSIONS

It was demonstrated that solution blow spinning is a simple method to easily obtain nanocomposites based on PVDF filled with MWCNT. These materials consisted of films formed by randomly interconnected fibers (mats) where the fibers have diameters below 400 nm. Optical microscopy, transmission electron microscopy and atomic force microscopy suggested that SBS is a good method to prepare nanocomposites with quite good dispersion of MWCNT within a PVDF polymer. In terms of stiffness, it was demonstrated that the incorporation of carbon nanotubes improves the mechanical

response of the PVDF at nanoscale, at least, when the PVDF based nanocomposites are processed in form of submicrometric fibers by SBS.

ACKNOWLEDGMENTS

This work was financial supported by the Projects MAT2014-59116-C2 (Ministerio de Economía y Competitividad); 2012/00130/004 (Fondos de Investigación de Fco. Javier Gonzalez Benito, política de reinversión de costes generales, Universidad Carlos III de Madrid) and 2011/00287/002 (Acción Estratégica en Materiales Compuestos Poliméricos e Interfases, Universidad Carlos III de Madrid). TEM characterization was made at LABMET, associated to the Red de Laboratorios de la Comunidad de Madrid. Finally, we would like to appreciate the technical support given by Carmen Ballesteros and Beatriz Galiana to perform the TEM test.

Conflict of Interest

The authors declare no conflict of interest.

REFERENCES

1. Song, F.; Koo, H.; Ren, D. Effects of material properties on bacterial adhesion and biofilm formation. *J. Dent. Res.* **2015**, *94*, 1027–1034.
2. Hidalgo-Bastida, L. A.; Barry, J. J. A.; Everitt, N. M.; Rose, F. R. A. J.; Buttery, L. D.; Hall, I. P.; Claycomb, W. C.; Shakesheff, K. M. *Acta Biomater.* **2007**, *3*, 457.

3. Kamimura, M.; Sugawara, M.; Yamamoto, S.; Yamaguchi, K.; Nakanishi, J. *Biomater. Sci.* **2016**, *4*, 933.
4. Huang, J.; Peng, X.; Xiong, C.; Fang, J. *J. Colloid Interface Sci.* **2011**, *355*, 503.
5. Brown, X. Q.; Ookawa, K.; Wong, J. Y. *Biomaterials* **2005**, *26*, 3123.
6. Yeung, T.; Georges, P. C.; Flanagan, L. A.; Marg, B.; Ortiz, M.; Funaki, M.; Zahir, N.; Ming, W.; Weaver, V.; Janmey, P. A. *Cell Motil. Cytoskeleton* **2005**, *60*, 24.
7. Tee, S. Y.; Fu, J.; Chen, C. S.; Janmey, P. A. *Biophys. J.* **2011**, *100*, L25.
8. Ingber, D. E. In *Principles of Tissue Engineering*; **2000**; pp 101.
9. Huang, Z. M.; Zhang, Y. Z.; Kotaki, M.; Ramakrishna, S. *Compos. Sci. Technol.* **2003**, *63*, 2223.
10. Reneker, D. H.; Yarin, A. L. Electrospinning jets and polymer nanofibers. *Polymer (Guildf)*. **2008**, *49*, 2387–2425.
11. Faraji, S.; Yardim, M. F.; Can, D. S.; Sarac, A. S. *J. Appl. Polym. Sci.* **2017**, *134*.
12. E.S. Medeiros, G.M. Glenn, A.P. Klamczynski, W.J. Orts, L. H. C. M. *J. Appl. Sci.* **2009**, *113*, 2322.
13. Dias, Y. J.; Gimenes, T. C.; Torres, S. A. P. V.; Malmonge, J. A.; Gualdi, A. J.; de Paula, F. R. *J. Mater. Sci. Mater. Electron.* **2018**, *29*, 514.
14. Sanchez, F. A.; González-Benito, J. *Polym. Compos.* **2015**.
15. Olmos, D.; Montero, F.; González-Gaitano, G.; González-Benito, J. *Polym. Compos.* **2013**, *34*, 2094.
16. Linghao He, Jing Sun, Xiaoli Zheng, Qun Xu, R. S. *Polym. Polym. Compos.* **2010**, *21*, 449.
17. Ribeiro, C.; Moreira, S.; Correia, V.; Sencadas, V.; Rocha, J. G.; Gama, F. M.; Gómez Ribelles, J. L.; Lanceros-Méndez, S. *RSC Adv.* **2012**, *2*, 11504.

18. Melorose, J.; Perroy, R.; Careas, S. *Nanomechanics of Materials and Structures*; **2015**; Vol. 1.
19. Chew, S. Y.; Hufnagel, T. C.; Lim, C. T.; Leong, K. W. *Nanotechnology* **2006**, *17*, 3880.
20. Yang, L.; Fitié, C. F. C.; van der Werf, K. O.; Bennink, M. L.; Dijkstra, P. J.; Feijen, J. *Biomaterials* **2008**, *29*, 955.
21. González-Benito, J.; Teno, J.; González-Gaitano, G.; Xu, S.; Chiang, M. Y. *Polym. Test.* **2017**, *58*, 21.
22. Navidfar, A.; Azdast, T.; Karimzad Ghavidel, A. *J. Appl. Polym. Sci.* **2016**, *133*.
23. Kracke, B.; Damaschke, B. **2012**, *361*, 10.

Figures

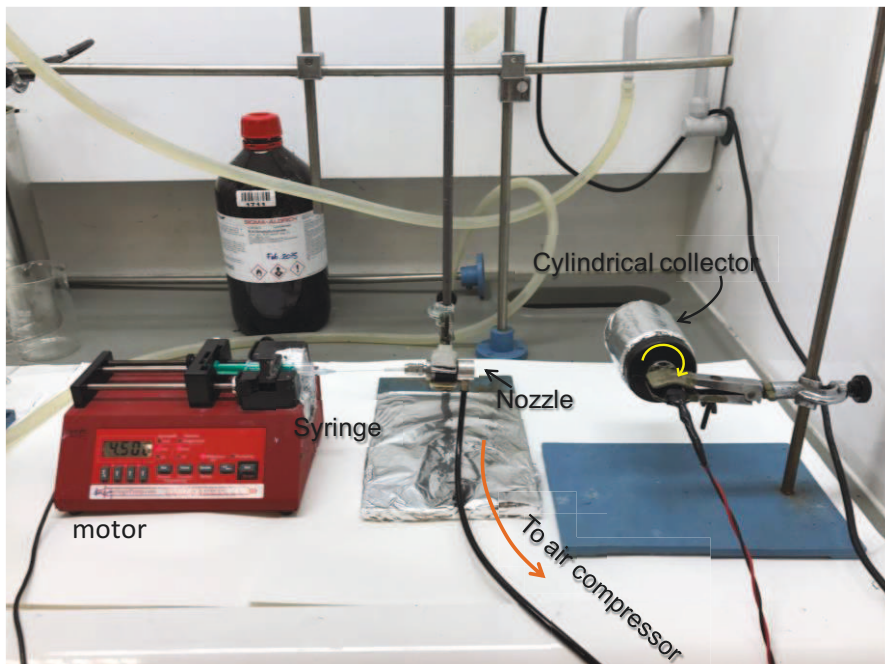


Figure 1.

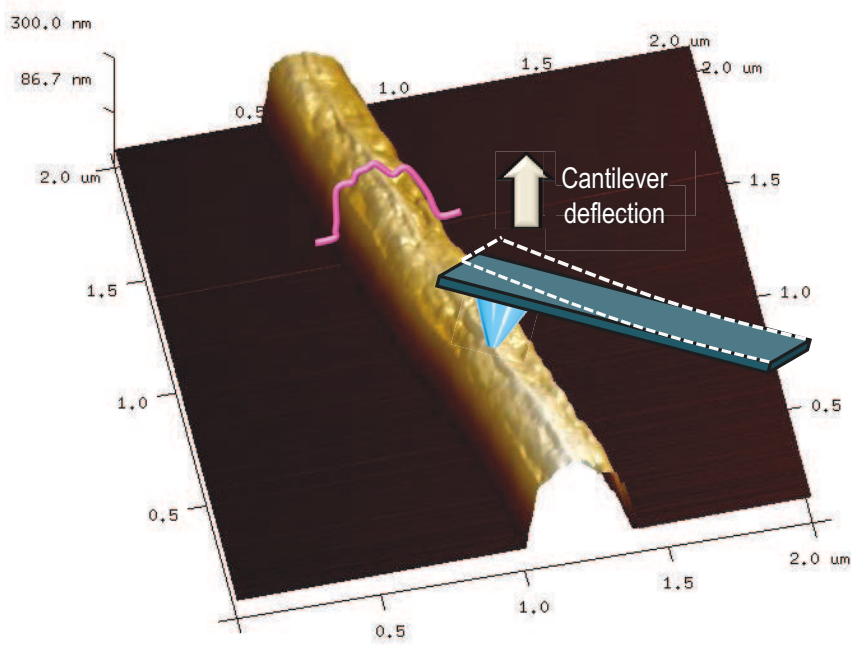


Figure 2.

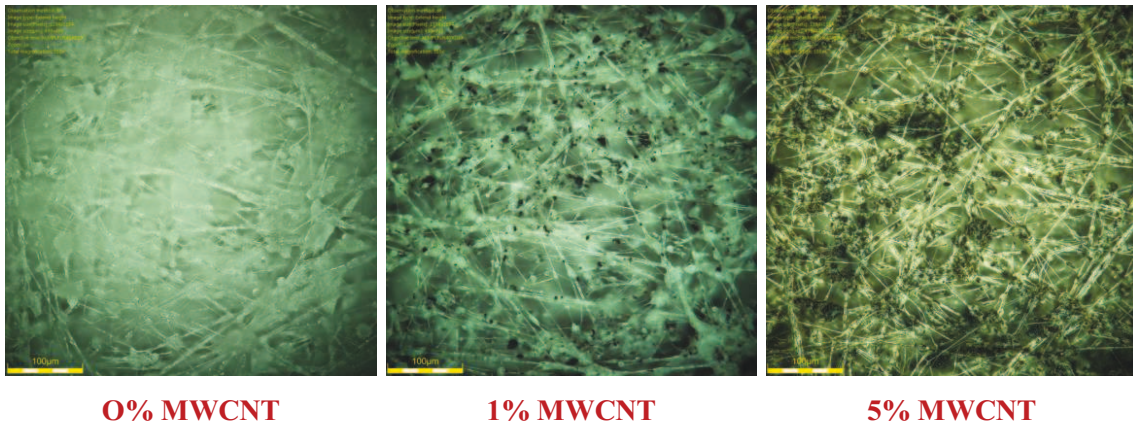


Figure 3.

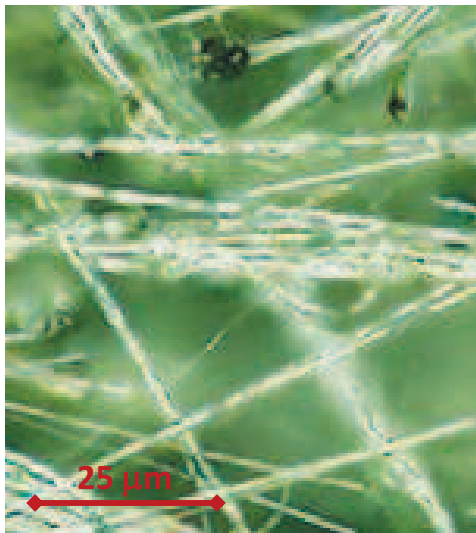


Figure 4.

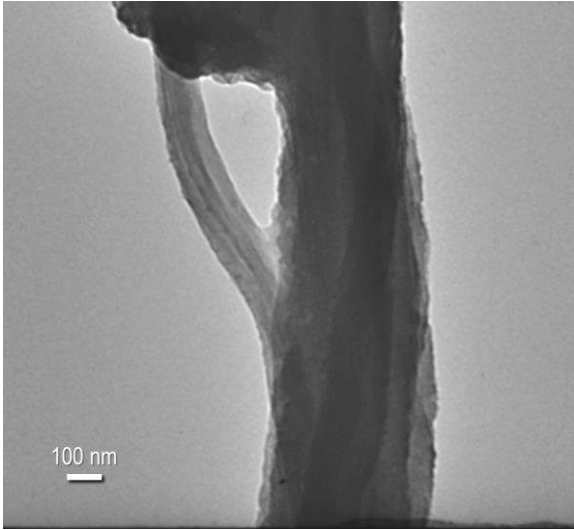


Figure 5.

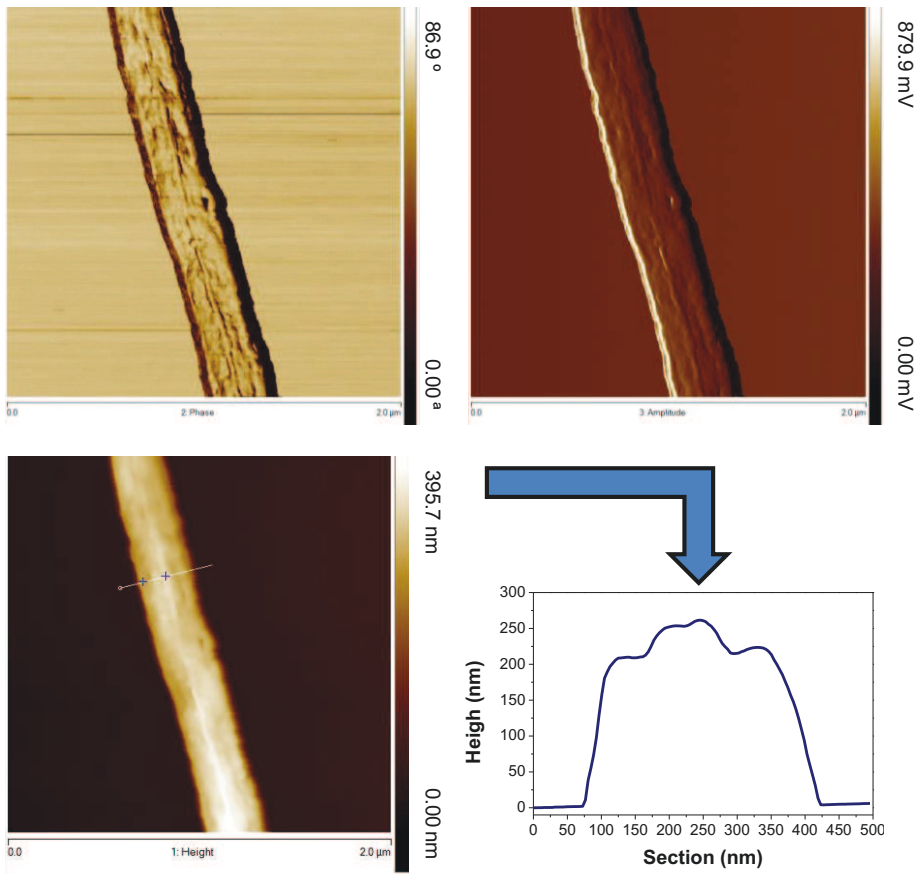


Figure 6.

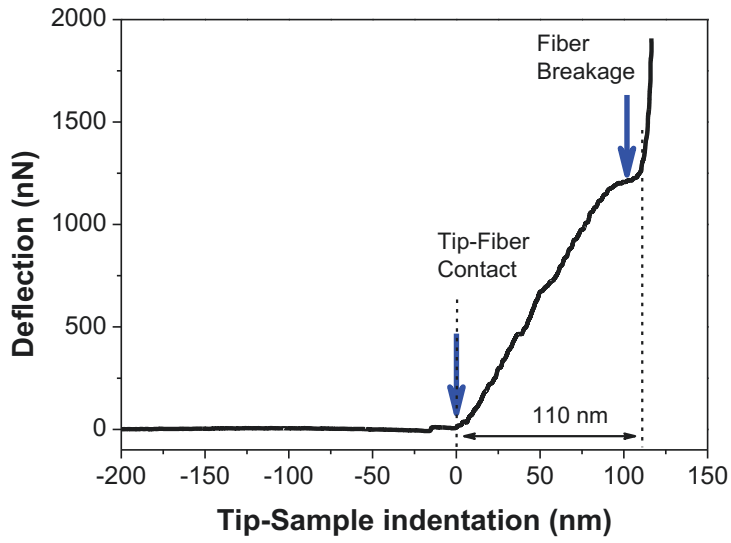


Figure 7.

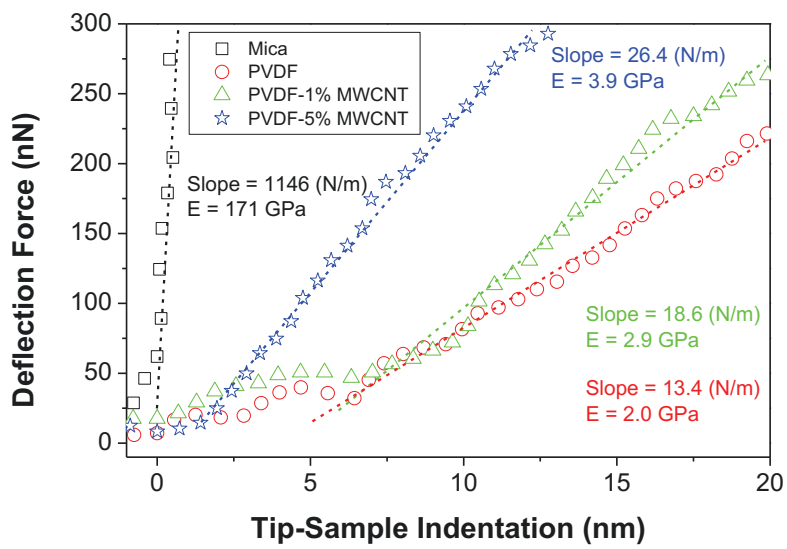


Figure 8.

Tables

Table 1. Topographical parameters obtained from fibers of the SBS materials under study.

Sample	R_{max} (nm)	R_z (nm)	R_{ms} (nm)	R_a (nm)
PVDF	31	5	8	6
PVDF- 1%MWCNT	36	9	10	7
PVDF- 5%MWCNT	46	12	9	7

Figure Captions

Figure 1. Picture of the experimental setup used to produce samples by solution blow spinning.

Figure 2. Example of topographic image of a blow spun fiber (PVDF + 1% of MWCNT) showing schematically the position of the tip to perform the indentation test.

Figure 3. Optical images of solution blow spun PVDF based samples.

Figure 4. Zoomed region of the image for the sample with 5% by weight of MWCNT.

Figure 5. TEM image showing part of a PVDF fiber filled with 1% by weight of MWCNT.

Figure 6. Example of AFM images, phase (top-left) contrast, amplitude (top-right) and heights (bottom-left); so as a cross section profile for a fiber of the composite based on PVDF filled with 1% wt of MWCNT obtained by SBS (bottom-right).

Figure 7. Example of a typical indentation force curve obtained in a blow spun PVDF fiber.

Figure 8. Representative AFM indentation force curves (elastic part) of the PVDF based materials studied with different compositions in terms of MWCNT.

GRAPHICAL ABSTRACT

The method so called **solution blow spinning** is used to obtain **submicrometric fibers based on poly(vinylidene fluoride), PVDF**, being able of loading them with **multi-walled carbon nanotubes, MWCNT**, well dispersed within the polymer. Morphology and mechanical behavior are studied at nanoscale from **nanoindentation tests** to understand the influence of the presence of **MWCNT**.

